Gibbs–Curie–Wulff Theorem in Organic Materials: A Case Study on the Relationship between Surface Energy and Crystal Growth

*Rongjin Li, Xiaotao Zhang, Huanli Dong, Qikai Li, Zhigang Shuai, and Wenping Hu**

Gibbs considered that a crystal should, at equilibrium, take a form such that the total surface area times the surface free energy is at a minimum (heterogeneous phase equilibria theory). A crystal in this form is called the equilibrium crystal shape, which is unique at constant temperature and pressure. Then, Curie proposed that the normal growth rates of crystal faces are proportional to the surface free energies.[1] After that, Wulff stated that in equilibrium the central distances of the crystal faces from a point within the crystal (Wulff point) are proportional to the corresponding specific surface free energies of these faces, i.e., γ_i/h_i = constant (where γ_i is the specific surface free energy of crystal face i, and h_i is the central distance from Wulff point). This is the well-known Gibbs–Curie–Wulff theorem.[2] However, the lack of concrete experimental proof makes the theory imperfect at some degree. Moreover, there is little quantitative evidence to support this theorem in the field of organic materials, which actually limits its general acceptance and application as guidance on organic crystal engineering.[2b,c]

For inorganic materials, the crystal-forming components (atoms or ions) are spherical and there was no difference of the orientation when they were transported to the crystal phase during the crystal growth. However, for organic materials, the crystal-forming components (molecules) are composed of more than one atom and are typically not in the shape of a ball. The larger components make the crystal growth processes more complex than that of the inorganic materials and bring new questions, e.g., what is the orientation when they come into the crystal phase? Does this orientation obey the Gibbs–Curie–Wulff theorem?

Challenges to prove the Gibbs–Curie–Wulff theorem are located on the production of crystals in the equilibrium shapes, which requires the tuning of the crystal shape with the lowest surface free energy. Normally, components in crystals with covalent, ionic or metallic bonds stick together strongly when they collide, leaving little space for them to adjust their positions during the crystallization process.[3] Molecules in organic crystals are held together by week noncovalent interactions such as van der Waals forces or hydrogen bonding, which allows the molecules to move easily during crystallization, providing the convenience to study both the kinetic and dynamic progress of crystal growth. Moreover, organic crystals tend to exist as nanometer or micrometer sized "small" crystals,[4] and therefore can undergo rapid shape change to lower the total surface free energy, which provides another great merit for the investigation of crystallization.[5] From the experimental aspect, micro or nanometer sized organic crystals are indeed ideal systems to study the crystal growth progress to provide solid proof for the Gibbs–Curie–Wulff theorem.

Here, a heteroacene, dibenzo[*d*,*d*′]thieno[3,2-*b*;4,5-*b*′]dithiophene (DBTDT) is selected as a candidate to approach this scientific target. Single crystals with different morphologies were grown from the vapor phase and both the equilibrium crystal shapes and shape evolution routes were found to follow the Gibbs–Curie–Wulff theorem. Moreover, the packing mode of the organic molecules in the crystal was also discovered to abide by the principle of lowest total surface free energy. The findings provide concrete proof for the Gibbs–Curie–Wulff theorem and extend the theorem to organic material. The guidance of the theorem on organic materials will help to produce crystals with desired shape for a variety of purposes such as organic electronics, semiconductor industry, and biological science.

DBTDT was selected as the candidate because (i) it has no branch, thus the effect of side-chains could be neglected; (ii) it has no specific functional groups, as a result the formation of strong hydrogen bonds and dipole interactions can be neglected; (iii) the molecule exhibits ideal rigidity, in that sense the torsion of the molecules could be neglected. The simple structure of DBTDT makes it an ideal candidate for both experimental crystal growth and theoretical calculations. Moreover, it is a pentacene analogy, and possesses high ionization potential, high stability, high mobility, and can be easily synthesized at

Prof. R. Li, Dr. X. Zhang, Prof. W. Hu
Department of Chemistry
School of Science
Tianjin University and Collaborative Innovation Center of Chemical Science and Engineering (Tianjin)
Tianjin 300072, China
E-mail: huwp@tju.edu.cn
Prof. H. Dong, Prof. W. Hu
Beijing National Laboratory for Molecular Sciences
Institute of Chemistry
Chinese Academy of Sciences
Beijing 100190, China
Dr. Q. Li
School of Materials Science and Engineering
Tsinghua University
Beijing 100084, China
Prof. Z. Shuai
Department of Chemistry
Tsinghua University
Beijing 100084, China

DOI: 10.1002/adma.201504370

large scale.[6] These merits are highly valuable for its potential application in organic electronics.[7]

The phase diagram of a one-component system in *P–T* coordinates (see the Supporting Information, Figure S1) suggests two routes for the growth of organic crystals, from liquid (solution) and from vapor. We prefer the vapor route because (i) the vapor route could exclude the influence of possible contaminations from the solvents, etc. during the crystallization process; (ii) organic semiconductors exhibiting the highest performance, e.g., pentacene and rubrene, are always insoluble in common solvents,[8] and are therefore difficult to crystallize from solution; (iii) the quality of crystals from solution process can yet not challenge their vapor-grown counterparts.[9] A widely accepted method for the growth of high quality organic crystals by the vapor route is the physical vapor transport (PVT) technique (see the Supporting Information, Figure S2).[10] In our experiments, a quartz boat loaded with DBTDT powder was placed at the high-temperature zone and vaporized at 140 °C. Highly pure Ar was used as the carrier gas and the system was evacuated by a mechanical pump. Crystals of DBTDT nucleated spontaneously on octadecyltrichlorosilane modified SiO_2 wafers at a distance of 11.5–13.5 cm from the source material. The temperature decreases steadily to ambient temperature at the end of the furnace. The morphology of the crystal was examined using a field-emission scanning electron microscopy (SEM, Hitachi S-4300). Atomic force microscopy (AFM) measurements were carried out with a Nanoscope IIIa instrument (Digital Instruments). The crystal structure was analyzed by an X-ray diffraction system (XRD, Rigaku D/max 2500).

Typical SEM images of the crystals grown by PVT were shown in **Figure 1**. Three representative morphologies (i.e., hexagons, elongated hexagons, and diamonds) were observed in large area by controlling the growth temperature during the crystallization (other conditions were kept constant). Hexagonal structures (Figure 1a) were obtained by putting the crystal growth wafers closer to the material sublimation zone (≈11.5 cm away from the source, temperature at ≈100 °C), while a farer distance from the source (≈12.5 cm, temperature at ≈85 °C) would produce the elongated hexagonal crystals (Figure 1b), and an even farer distance (≈13.5 cm, temperature at ≈70 °C) would produce diamond-like crystals (Figure 1c). This method was facile for the controllable growth of organic crystals, and it would be useful for the crystallization of organic semiconductors with desired shapes.

XRD patterns of the crystals showed that all the samples of Figure 1a–c exhibited identical diffraction peaks regardless of their different appearances (Figure 1d), confirming that the as-grown crystals shared the same crystal structure along the direction of the substrate normal (see Figures S3 and S4 in the Supporting Information for analyses of the crystal structures within the substrate normal). The crystal shapes of DBTDT estimated by the Bravais–Friedel–Donnay–Harker (BFDH) method[11] were mainly hexagonal, which agreed well with our experimental results (Figure 1a). The elongated hexagonal crystals (Figure 1b) and diamond-like crystals (Figure 1c) were highly possible the evolved products of the hexagonal products (will be discussed later in the second to last paragraph). As shown in Figure 1d, the baseline of the XRD pattern was straight and

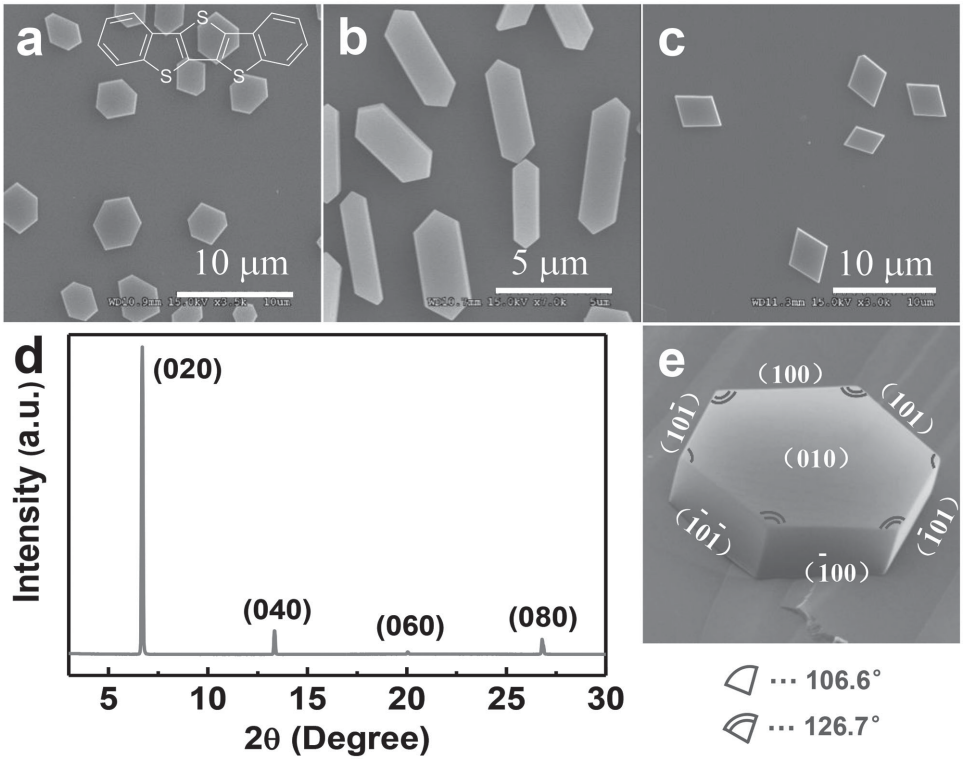

Figure 1. DBTDT crystals grown by physical vapor transport. a–c) SEM images of the crystals with hexagonal, elongated hexagonal, and diamond-like shape. d) A typical diffractogram of the crystals. e) An indexed crystal.

the diffraction peaks were strong and sharp, indicating the high quality of the crystals. There were four peaks present with multiple *d*-spacing. The primary diffraction peak (020) was at $2\theta = 6.70°$, corresponding to a *d*-spacing of 1.32 nm and equals half of the *b* axis (1.33 nm).[12] Only (0k0) reflections with even k numbers were observed in the diffractogram. The absence of the odd numbered reflections was a systematic absence due to the existence of 2_1 screw axes (parallel to the *b* crystallographic axes) in the crystal. In a symmetric reflection mode, the diffraction vector is perpendicular to the wafer plane and only the planes which lie parallel to the wafer can be probed. The absence of any other (hkl) reflections of our DBTDT crystals indicated that the as-grown crystals were oriented with their (0k0) planes parallel to the substrate. Hence, the largest plane of the hexagonal crystals was (010), which should be parallel to the substrates. Moreover, according to Steno's law (the law of the constancy of interfacial angles) and the regular hexagonal shape of the crystals, the faceted angles of 106.6° and 126.7° in the basal (010) plane were calculated to be the interfacial angles between the lateral (100), (101), (–101), (–100), (–10–1), and (10–1) planes (Figure 1e).

According to the Gibbs–Curie–Wulff theorem, the equilibrium shape of a crystal is closely related with the free energy of the corresponding crystal surfaces. Hence, the surface free energies of DBTDT crystal were calculated carefully by molecular dynamics taking into accounts both the internal energy and the entropy contributions using a method developed by Marcon and Raos[13] (see the Supporting Information, Figure S5, for the details). The calculated surface energies corresponding to the (001), (010), (100), (101), and (10–1) surfaces were displayed in **Table 1**. Wulff construction viewing along the *b* crystallographic direction was sketched based on the calculated results (**Figure 2**a). It was obvious that the surface free energy of (010) was the lowest, i.e., growing the slowest, and the largest plane of the crystal should be (010). It agreed accurately with our experimental results as shown in Figure 2b. The other 3 surfaces (101), (–101), and (100) possessed surface free energies with small differences (<2%), indicating the growth rates of DBTDT molecules in these directions were not much different. The surface free energy of (001) was higher than that of the above mentioned surfaces and this plane should not appear in Wulff construction. This was indeed the case in our experimental products. Certainly, other high-index plane should have much higher surface free energies and they should not belong to the equilibrium shape too. Figure 2c sketched the Wulff construction viewing at about 45° angle from the *b* direction. Judging from the SEM image of Figure 2d, the grown crystal resembles the sketch exactly. The morphological accordance

Table 1. The calculated surface energies at 400 K.

Surface	γ [mJ m^{-2}]	γ_i/γ_{010}
(010)	19.49	1.00
(101)	37.33	1.92
(–101)	37.08	1.90
(100)	37.97	1.95
(001)	43.66	2.24

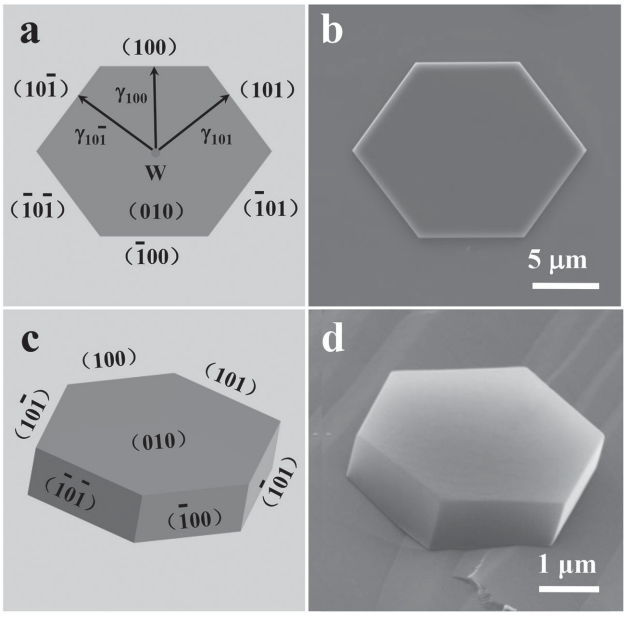

Figure 2. Equilibrium crystal shapes predicted by the Gibbs–Curie–Wulff theorem and the corresponding SEM images of the crystals grown by PVT. a) Wulff construction of DBTDT crystal viewing along the *b* direction. The *i*th central distance from Wulff point *W* represents surface free energy γ_i at 400 K. b) SEM image of a representative hexagonal crystal viewing along the *b* direction. c) Wulff construction viewing at about 45° angle from the *b* direction. d) SEM image of a representative hexagonal crystal viewing at about 45° angle from the *b* direction.

of our grown crystals and the equilibrium forms predicted by Gibbs–Curie–Wulff theorem provided concrete proof for the theory.

Principally, there are two accepted mechanisms for the growth of the (010) surface: spiral growth around a dislocation and surface nucleation followed by 2D growth.[14] As for the orientation of DBTDT molecules in the (010) surface, three are two possibilities: parallel (lying-down mode) or perpendicular (standing-up mode) to the substrates. To investigate the mechanism and packing mode of DBTDT in the crystal, AFM measurements were performed. An AFM image obtained on the (010) surface was shown in **Figure 3**a. Three molecular layers can be seen clearly, indicating that the mechanism of growth is surface nucleation followed by 2D growth. A growing layer from the (010) surface of the crystal was shown in Figure 3b, and the enlarged image of the selected part was shown in Figure 3c. Based on the section analysis (points A, B, and C), it was obvious that the height of the step on the (010) crystal surface was ≈1.3 nm, which was very close to the length of the DBTDT molecule (1.26 nm), indicating the fact that the DBTDT molecules tend to pack perpendicularly to the substrates. XRD measurements of the DBTDT layers indicated a *d*-spacing of 1.32 nm, which was equal to half of the *b* axis and coincides well with the AFM analysis.

The layer-by-layer 2D growth mechanism and the standing-up packing mode of DBTDT molecules in the crystal was depicted in the lower part of Figure 3d. With the rigid linear DBTDT molecules standing up on the substrate, the

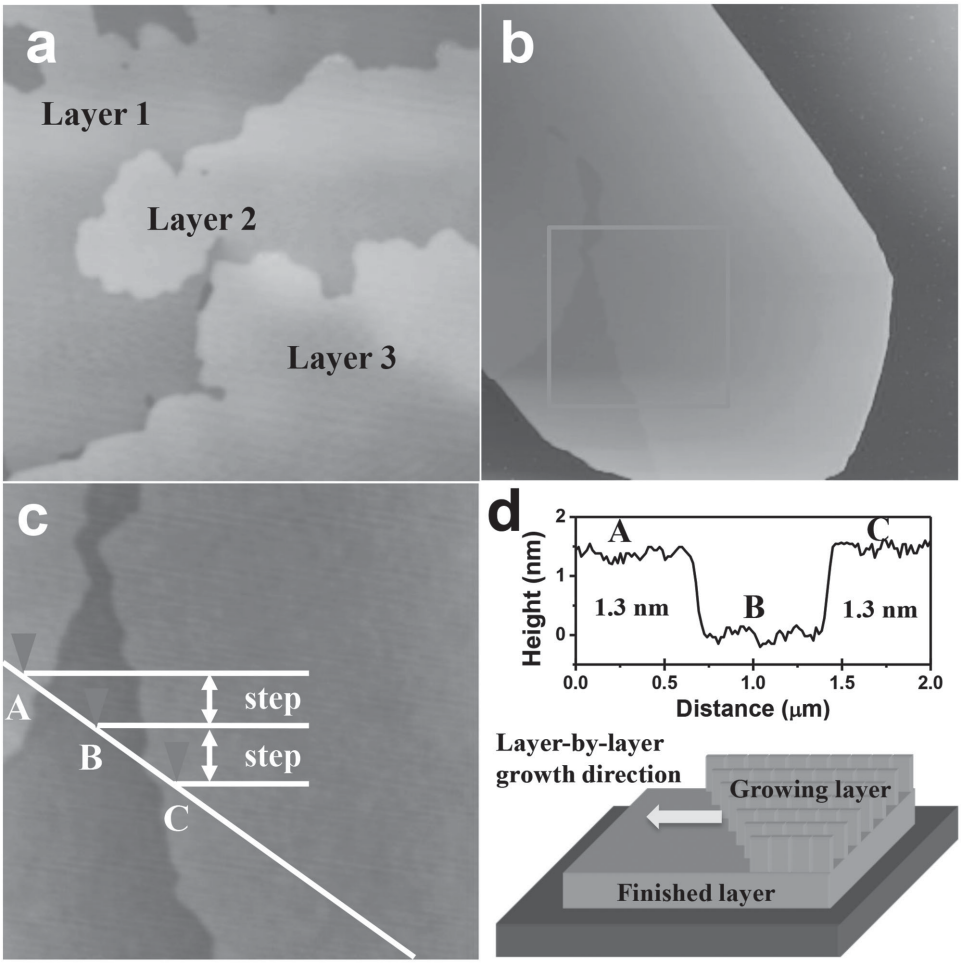

Figure 3. The layer-by-layer growth mode of DBTDT crystals according to Gibbs–Curie–Wulff theorem. a) AFM image of the layers on the surface of one DBTDT crystal. b) AFM image of a growing crystal of DBTDT. c) The enlarged image of the selected part in (b) containing growth steps. d) The section analysis of the step in (c). The step height was ≈1.3 nm, which was near the length of DBTDT molecule, confirming that the crystal grew in a layer-by-layer mode with DBTDT molecule packed perpendicularly to the substrates.

layer-by-layer growth model minimizes the surface energy due to the rather weak H—H interlayer interactions in the *b* crystal direction. Clearly, stacking perpendicular to the substrates was the best way to keep the system with the lowest surface free energy.[15] Such way of growth stood well with the Gibbs–Curie–Wulff theorem. Except DBTDT, many other organic molecules also adopt the standing-up mode.[16] A well-known fact is that the packing mode of molecules in the solids is crucial for organic optoelectronic devices.[17] The Gibbs–Curie–Wulff theorem provided a clue to understand the origin of molecular packing and the related optoelectronic properties, which was beneficial for the examination of the detailed growth mechanism of crystals and the controllable growth of molecular crystals for high performance devices.[18]

Finally, as a distinguished part of the Gibbs–Curie–Wulff theorem, the prediction of the evolution of crystal shapes (the lateral growth) is indivisible. As shown in Table 1, the six lateral planes of DBTDT crystals exhibited small difference in specific surface free energy. Therefore, according to the Gibbs–Curie–Wulff theorem, any of the six lateral planes had a chance to grow under slightly different conditions, such as the fluctuation of temperature, pressure, or gas flow rate. Indeed, crystals with the growth of one to six lateral planes were found in the products and some of the examples were exemplified in **Figure 4**. The crystals can grow by any route from 1 to 6, i.e., the growth from one lateral plane to six lateral planes simultaneously. For example, the symmetrical growth of planes (100) and (–100) would result in the formation of diamond-like crystals with interior angels of 73.4° (route 2), while the symmetrical growth of plane (101), (–101), (–10–1), and (10–1) would produce elongated hexagonal crystals (route 4). The possibility of route 2 and route 4 explained the production of diamond-like and elongated hexagonal crystals shown in Figure 1 b,c. If the six lateral planes grew at rates following the Gibbs–Curie–Wulff Theorem, larger hexagonal crystals would be produced (route 6).

In summary, direct proof of the Gibbs–Curie–Wulff theorem is provided by the controllable growth of organic crystals. The equilibrium crystal shape of DBTDT consists well with the

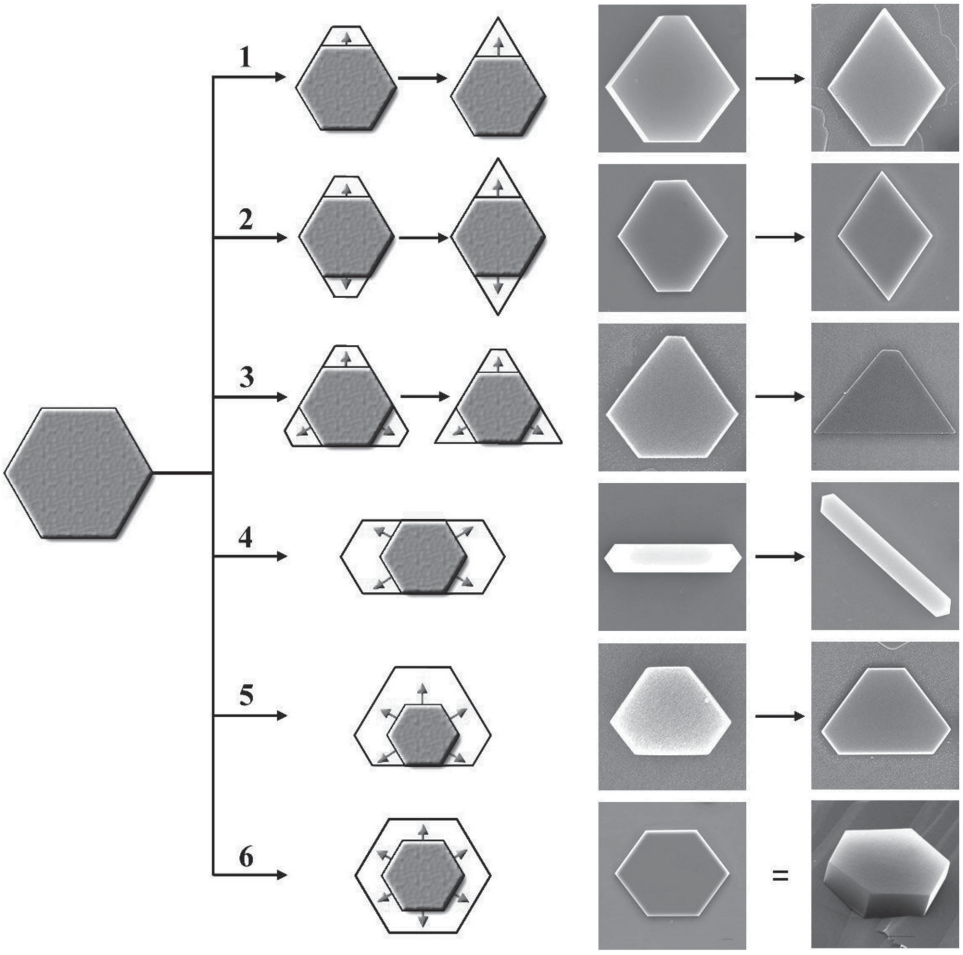

Figure 4. The evolution of crystal shapes (the lateral growth) according to Gibbs–Curie–Wulff theorem. Here, six routes were demonstrated, i.e., the growth could start from 1, 2, 3, 4, 5, or 6 lateral planes of the crystal. With these growth possibilities, the final crystal shape would evolve into the shapes as sketched in the left-hand side and SEM images of the as-grown products were shown in the right-hand side.

morphology predicted by the Gibbs–Curie–Wulff theorem. The surface free energies play essential roles in the crystal growth progress and determine the orientation of the molecules in the crystals. An in-depth study on the crystallization of organic crystals may open the perspective toward further understanding of organic thin-film and crystal growth dynamics and promote their applications in organic electronics.

Supporting Information

Supporting Information is available from the Wiley Online Library or from the author.

Acknowledgements

The authors greatly thank Prof. Keqiu Chen (Hunan University) for the theoretical discussion. This work was supported financially by the National Natural Science Foundation of China (Grant Nos. 51222306, 91222203, 91233205, and 91433115), the Ministry of Science and Technology of China (Grant Nos. 2011CB808405, 2011CB932304, 2013CB933403, and 2013CB933504), the Chinese Academy of Sciences (Grant No. XDB12030300), and the Youth Innovation Promotion Association CAS.

Received: September 6, 2015
Revised: October 28, 2015
Published online: December 17, 2015

[1] M. P. Curie, *Bull. Soc. Min. Fr.* **1885**, *8*, 145.
[2] a) G. Wulff, *Z. Kristallogr. Mineral.* **1901**, *34*, 449; b) I. V. Markov, *Crystal Growth for Beginners: Fundamentals of Nucleation, Crystal Growth and Epitaxy*, World Scientific Publishing Co. Pte. Ltd., Singapore **1995**; c) J. W. Mullin, *Crystallization*, Butterworth-Heinemann, Oxford, UK **2001**.
[3] I. Sunagawa, *Crystals Growth, Morphology, and Perfection*, Cambridge University Press, NY, USA **2005**.
[4] R. Li, W. Hu, Y. Liu, D. Zhu, *Acc. Chem. Res.* **2010**, *43*, 529.
[5] G. M. Whitesides, B. Grzybowski, *Science* **2002**, *295*, 2418.
[6] a) J. Gao, R. Li, L. Li, Q. Meng, H. Jiang, H. Li, W. Hu, *Adv. Mater.* **2007**, *19*, 3008; b) R. Li, L. Jiang, Q. Meng, J. Gao, H. Li, Q. Tang, M. He, W. Hu, Y. Liu, D. Zhu, *Adv. Mater.* **2009**, *21*, 4492.

[7] a) V. Podzorov, *MRS Bull.* **2013**, *38*, 15; b) A. Yassar, *Poly. Sci. Ser. C* **2014**, *56*, 4.
[8] C. Reese, Z. Bao, *Mater. Today* **2007**, *10*, 20.
[9] H. Moon, R. Zeis, E. J. Borkent, C. Besnard, A. J. Lovinger, T. Siegrist, C. Kloc, Z. Bao, *J. Am. Chem. Soc.* **2004**, *126*, 15322.
[10] a) C. Kloc, P. G. Simpkins, T. Siegrist, R. A. Laudise, *J. Cryst. Growth* **1997**, *182*, 416; b) R. A. Laudise, C. Kloc, P. G. Simpkins, T. Siegrist, *J. Cryst. Growth* **1998**, *187*, 449.
[11] a) A. Bravais, *Études Cristallographiques*, Academie des Sciences, Paris, France **1913**; b) J. D. H. Donnay, D. Harker, *Am. Min.* **1937**, *22*, 446.
[12] T. Okamoto, K. Kudoh, A. Wakamiya, S. Yamaguchi, *Org. Lett.* **2005**, *7*, 5301.
[13] V. Marcon, G. Raos, *J. Am. Chem. Soc.* **2006**, *128*, 1408.
[14] R. L. Penn, J. F. Banfield, *Science* **1998**, *281*, 969.
[15] D. Nabok, P. Puschnig, C. Ambrosch-Draxl, *Phys. Rev. B* **2008**, *77*, 245316.
[16] a) M. A. Loi, E. Da Como, F. Dinelli, M. Murgia, R. Zamboni, F. Biscarini, M. Muccini, *Nat. Mater.* **2005**, *4*, 81; b) F. Heringdorf, M. C. Reuter, R. M. Tromp, *Nature* **2001**, *412*, 517; c) H. Minemawari, T. Yamada, H. Matsui, J. Tsutsumi, S. Haas, R. Chiba, R. Kumai, T. Hasegawa, *Nature* **2011**, *475*, 364.
[17] a) H. Sirringhaus, P. J. Brown, R. H. Friend, M. M. Nielsen, K. Bechgaard, B. M. W. Langeveld-Voss, A. J. H. Spiering, R. A. J. Janssen, E. W. Meijer, P. Herwig, D. M. de Leeuw, *Nature* **1999**, *401*, 685; b) H. Sirringhaus, *Adv. Mater.* **2014**, *26*, 1319; c) P. M. Beaujuge, J. M. J. Frechet, *J. Am. Chem. Soc.* **2011**, *133*, 20009.
[18] a) W. K. Burton, N. Cabrera, F. C. Frank, *Nature* **1949**, *163*, 398; b) H. J. Scheel, T. Fukuda, *Crystal Growth Technology*, William Andrew Inc., New York **2003**; c) C. Reese, Z. Bao, *J. Mater. Chem.* **2006**, *16*, 329.